DOI: 10.2478/ata-2026-0002

Acta Technologica Agriculturae 1
Nitra, Slovaca Universitas Agriculturae Nitriae, 2026, pp. 7–17

DESIGN OF A LOW-COST ROBOTIC PROTOTYPE FOR FRUIT HARVEST WITH FLEXIBLE GRIPPING USING 3D PRINTING

Maxwell SALAZAR*, Paola PORTERO, Santiago PÉREZ

Instituto Tecnológico Superior Rumiñahui, Research Department, Electronic Department, Sangolquí, Ecuador,
paola.portero@ister.edu.ec (P.P.), santiago.perez@ister.edu.ec (S.P.)

*correspondence: maxwell.salazar@ister.edu.ec

The accelerating demand for food production driven by economic, political, and social factors has highlighted the need for innovative solutions to increase harvesting efficiency. In response, this work presents the design and development of a prototype robotic arm for fruit harvesting, suitable for medium-sized fruits such as citrus, apples, and pears in semi-controlled environments like greenhouses and experimental orchards. The system integrates four Nema 17 stepper motors (17HS8401) and four 360-degree servomotors (MG996R), structured as a three-degree-of-freedom mechanism to balance simplicity and functionality, enabling easy replication. The arm components were fabricated using 3D printing technology, combining rigid polylactic acid filament for structural parts and flexible thermoplastic polyurethane filament for the adaptive gripper. The unique design eliminates the need for sensors, allowing adaptable and reliable fruit collection using cost-effective actuation while minimising damage to delicate produce. Experimental validation showed success rates of 87% for citrus fruits, 67% for apples, and 60% for pears, highlighting the system's adaptability to different fruit geometries and textures. Comprehensive force and torque calculations ensure the system's operational viability despite relying on low-cost electronic components. These findings demonstrate that the proposed robotic solution offers a practical, low-cost, and adaptable approach for agricultural automation, bridging the gap between laboratory prototypes and deployable systems for small- and medium-scale producers.

Keywords: agricultural automation; soft robotics; flexible materials; low-cost electronics

Within Agriculture 4.0 technology, the development of robotic harvesting systems represents a challenge for researchers. These systems must adapt to many conditions due to the variety of foods to be harvested, in addition to the care required for delicate products whose quality must be preserved (Navas et al., 2024). Conventional harvesting depends on human labour, and although there are automated systems, these work with specific crops that allow the use of heavy machinery. However, harvesting is still carried out manually in a time-consuming, monotonous, and costly process that depends on seasonal labour (Magistri et al., 2024). As the demand for fresh produce increases, it is evident that automation will play a crucial role in supplying the required crops (Alaaudeen et al., 2024).

Recent studies indicate that current robotic harvesting solutions typically achieve success rates between 55% and 75%, depending on crop type, sensing strategy, and environmental conditions (Navas et al., 2024; Elfferich et al., 2022). Quantifying these performance levels is essential to contextualise the contribution of the present work, which aims to provide a competitive or improved success rate through a simpler and more cost-effective approach (Kashkarov et al., 2018).

The greatest difficulty in fruit harvesting is the variety of fruits. They come in different sizes, shapes, and textures, making it impossible to unify the harvesting into a single process, as it must be done without damaging the fruit (Bac et al., 2014). Robotic grippers are typically made of hard materials such as steel or aluminium, which, although useful in industry, destroy fruit due to their inability to adapt. Grippers must also be adapted using complex algorithms or specialised sensors to improve efficiency (Spagnuolo et al., 2025). To solve this, soft robotics uses flexible materials to construct elements that adapt to different fruits without excessive complexity, reducing the likelihood of damage (Hasanshahi et al., 2024).

The improvement in 3D printing now allows the construction of low-cost robotic systems. It is possible to manufacture a flexible gripper using thermoplastic polyurethane (TPU), a material that provides the necessary flexibility and strength to harvest without damaging the product (Zhang et al., 2024). With this material, prototypes can be built to adapt to different conditions, allowing for adjustment at each stage of design and construction (Afsah-Hejri et al., 2022).

Small and medium-sized agricultural producers often face limitations in adopting robotic solutions due to high equipment costs and technical complexity (Elfferich et al., 2022). While several commercial systems exist, most are tailored for large-scale operations, creating a gap in solutions accessible to low-resource environments. Recent developments in 3D printing and soft robotics provide new pathways for addressing this issue (Navas et al., 2024). According to a review by De Grandpré et al. (2022), automatic harvesting systems are increasingly incorporating vision-based recognition and flexible mechanisms to reduce fruit damage and improve adaptability. However, many current systems still lack the balance between efficiency, affordability, and simplicity required for real-world deployment in orchards and greenhouses. This highlights the need for cost-effective, easy-to-build solutions like the one proposed in this study (Genbach et al., 2018).

In this research, not only is the gripper important; the arm complements the robotic system, which must be precise, reliable, and easy to build. A three-degree-of-freedom arm powered by Nema 17 stepper motors was chosen. These are inexpensive and ideal for providing controlled and repeatable movements (An et al., 2022). The gripper moves using nylon cables pulled by four 180-degree servomotors, allowing it to adapt to any fruit (Baur and Iles, 2023). The article includes calculations to validate the use of these motors. Although inexpensive, if used properly, they can meet the harvesting objective in controlled situations.

The research aims to contribute to agricultural automation by presenting a low-cost robotic arm adaptable to different fruits. Leveraging 3D printing, the arm can be adapted to various situations with minimal changes, and the design is scalable for larger prototypes (Davidson et al., 2016). Statistical calculations determine the viability of the robot, allowing for future adjustments for real implementation, paving the way for increased automation in agriculture (Elfferich et al., 2022).

The proposed robotic system is intended for use in semi-controlled environments such as greenhouses or experimental orchards, where accessibility and fruit location are predictable and where terrain and weather conditions can be regulated.

Material and Methods

The robotic arm prototype was built in stages, from identifying necessary characteristics, designing, constructing, and testing components, to obtaining a functional prototype. The parts were modelled for easy editing to allow refinement and ensure compatibility between mechanical and electronic elements (Davidson et al., 2016). The arm's movement is achieved by transmitting motor force through toothed belts similar to 3D printers. As a prototype, testing was limited to controlled environments, with fruit positioned manually.

Mechanical design of the robotic arm

The prototype consists of a 360-degree rotating base, a main arm lifted by two parallel motors, and a secondary arm, to which the flexible gripper is connected. This assembly allows the fruit to be reached and manipulated within a controlled ecosystem. The prototype focuses on structural balance and manoeuvrability, ensuring efficient handling. Figure 1 illustrates the general structure of the robotic arm and its key mechanical components.

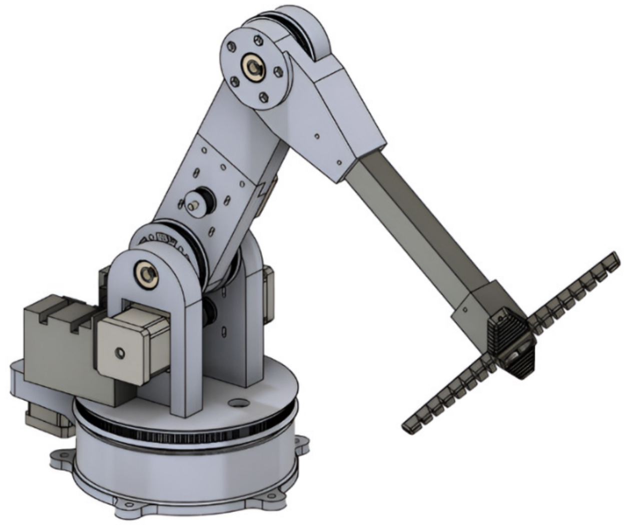

Fig. 1 Complete robotic arm design

Although Cartesian and SCARA manipulators are commonly used in industry, articulated arms offer greater flexibility in constrained environments. Given the variability in plant structure and fruit location, a 3DOF articulated design was chosen for its balance between manoeuvrability, simplicity, and ease of replication.

The robotic arm structure was manufactured with polylactic acid (PLA), selected for its ease of printing and lightness. Additive 3D printing allowed for rapid prototype construction and component modification (Harman and Sklar, 2022). The secondary arm is made of aluminium, guaranteeing greater structural strength. The aluminium secondary arm was chosen for its rigidity and load-bearing capacity, while PLA was used in the main structure for lightweight construction and ease of prototyping. Both materials are joined with M4 screws and printed brackets, allowing rapid disassembly, modular replacement, and low-cost repairs – critical advantages for iterative testing and adaptation to different crops. The motors provide precise position control and sufficient force to ensure movement (Buzzatto et al., 2024). This set of elements, whose technical parameters are detailed in Table 1, results in an arm with controlled movements and precision adequate for the first prototype. For a better understanding, Fig. 2 shows a dedicated diagram illustrating the manipulator's joint arrangement (base rotation, main arm elevation, secondary

Table 1 Technical parameters of the arm

Parameter	Value
Maximum reach	520 mm
Base rotation	360°
Main arm lift	0° - +120°
Secondary arm lift	-45° - +45°
Estimated maximum load	200 g (including fruit)
Structural material	PLA and aluminium

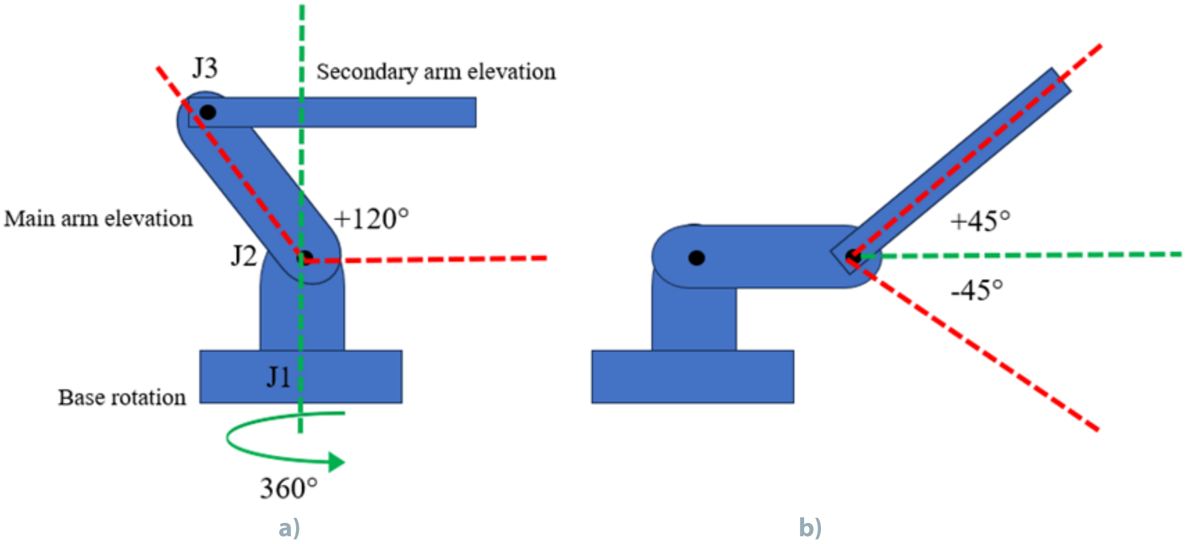

Fig. 2 The possible range of motion for the prototype robotic arm: a) 360 rotations of the base and the tilt of the main arm; b) the manoeuvrability of the secondary arm

arm tilt), including link lengths and angular ranges. This visualisation supports the workspace analysis and demonstrates the operational envelope for fruit harvesting.

Degrees of freedom and transmission system

Three degrees of freedom were selected to maintain a balance between mechanical complexity and task requirements. This configuration allows for vertical and horizontal positioning, as well as depth adjustment, covering a practical operational envelope for fruit harvesting. To achieve precise control, the joints are rotated using pulleys and timing belts. This design increases the power of the NEMA 17 motors and improves movement efficiency. The motor pulleys are commercially available, and the complementary pulleys are constructed from PLA. Simply changing the pulleys changes the transmission ratio, increasing the effective output torque and improving performance. As shown in Fig. 3, the distribution of the arm components is explained below.

Kinematic modelling of the robotic arm

To provide a theoretical foundation for the robotic arm's operation, a simplified kinematic description was performed using the Denavit–Hartenberg (D-H) convention. The manipulator has three degrees of freedom (DOF):

1. Joint 1 (θ_1, base rotation): revolute joint allowing rotation about the vertical axis.
2. Joint 2 (θ_2, main arm elevation): revolute joint controlling the vertical movement of the main arm.
3. Joint 3 (θ_3, secondary arm tilt): revolute joint adjusting the tilt of the secondary arm for fruit grasping.

The parameters of the manipulator, based on the D-H convention, are summarised in Table 2.

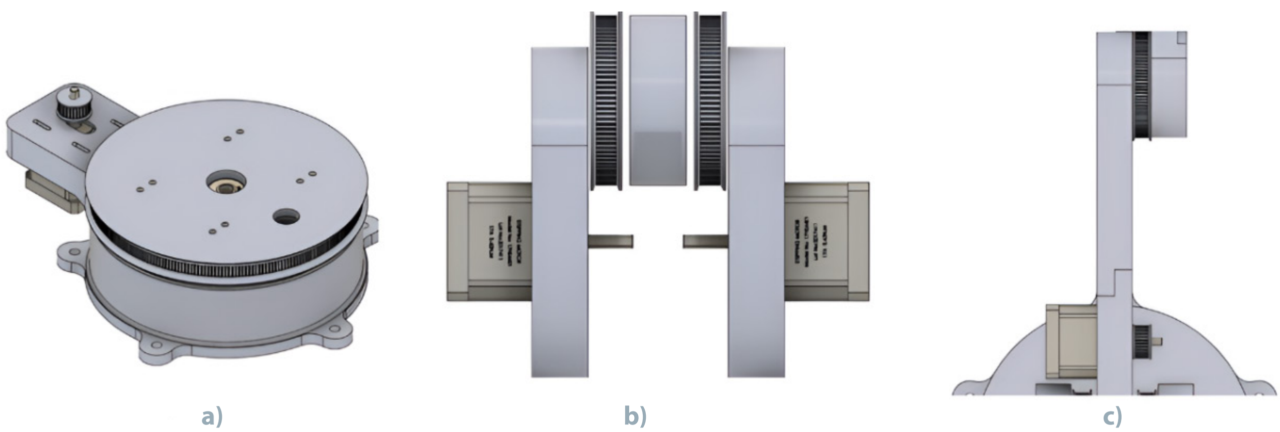

Fig. 3 a) A single Nema 17 motor rotates the robotic arm in the horizontal plane, allowing a 360-degree rotation; b) Two Nema 17 motors are used in parallel, facing each other, ensuring sufficient torque to initiate movement with or without load; c) A motor controls the secondary elevation of the robotic arm, ensuring optimal positioning

Table 2 D-H parameters of the prototype

Joint (i)	θ_i (variable)	d_i (offset)	a_i (link length)	α_i (twist)
1	θ_1	0	L_1 = 100 mm	90°
2	θ_2	0	L_2 = 280 mm	0°
3	θ_3	0	L_3 = 250 mm	0°

Using the standard homogeneous transformation matrices:

$$T(i-1 \to i) = \begin{bmatrix} \cos\theta_i & -\sin\theta_i \cdot \cos\alpha_i & \sin\theta_i \cdot \sin\alpha_i & a_i \cdot \cos\theta_i \\ \sin\theta_i & \cos\theta_i \cdot \cos\alpha_i & -\cos\theta_i \cdot \sin\alpha_i & a_i \cdot \sin\theta_i \\ 0 & \sin\alpha_i & \cos\alpha_i & d_i \\ 0 & 0 & 0 & 1 \end{bmatrix}$$

The overall forward kinematics of the manipulator is expressed as:

$$T = T(0 \to 1) \times T(1 \to 2) \times T(2 \to 3)$$

where: T – provides the position and orientation of the gripper relative to the base coordinate frame

This formulation allows characterisation of the workspace and serves as the basis for solving inverse kinematics in future developments, which will be relevant for improving accuracy and automated trajectory planning.

To complement the mathematical formulation, Fig. 4 presents the kinematic scheme of the proposed manipulator, showing the link lengths (L_1, L_2, L_3) and the revolute joints (θ_1, θ_2, θ_3).

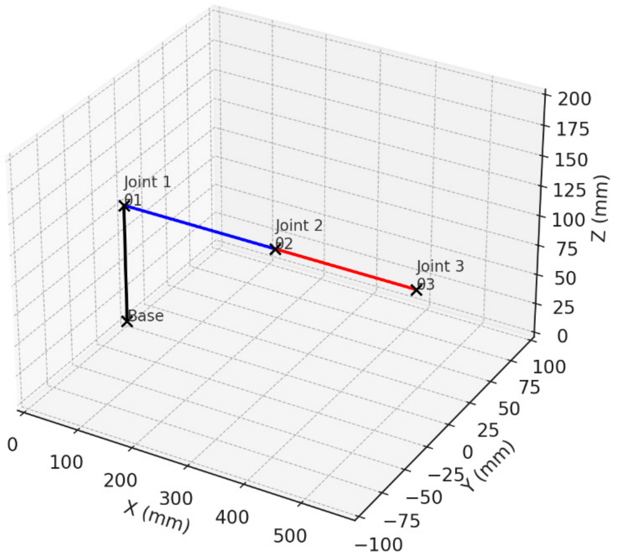

Fig. 4 Kinematic scheme of the 3-DOF robotic arm using the Denavit–Hartenberg model

The diagram shows the base height (L_1), the main arm (L_2), and the secondary arm (L_3), together with the revolute joints (θ_1, θ_2, θ_3). This representation defines the link parameters used for the forward kinematics analysis.

Modular secondary arm and adaptability

The secondary arm was designed using an interchangeable square aluminium profile (Fig. 5), allowing its length to be adjusted according to the specific requirements of different harvest environments. This modular approach enhances the system's adaptability to various crop types and plant heights. The material selected for the prototype's construction was designed to achieve a balance between structural strength and lightweight design. Figure 6 shows the final result of the prototype.

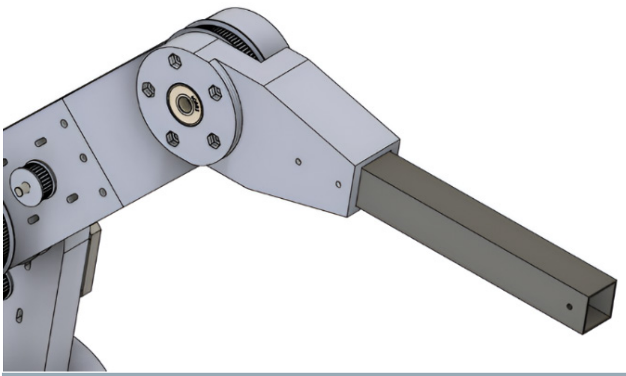

Fig. 5 The end of the arm made up of a square aluminium profile attached with screws to the plastic structure

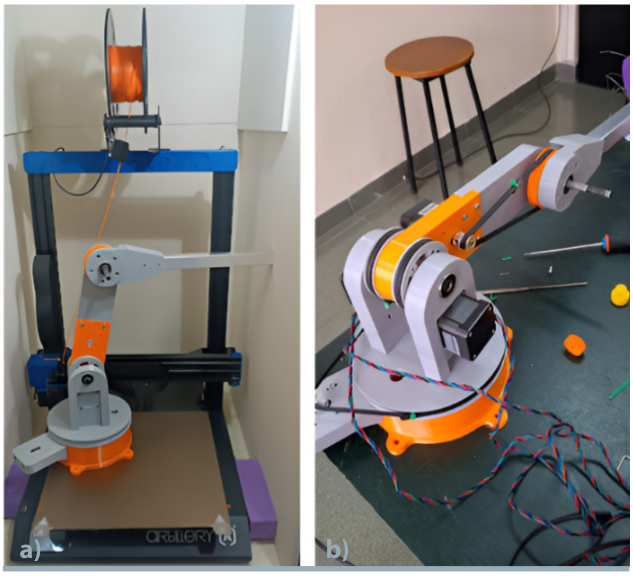

Fig. 6 The prototype built using 3D printing: a) The complete structure in PLA plastic; b) The positioning of the belts and motors used for the prototype

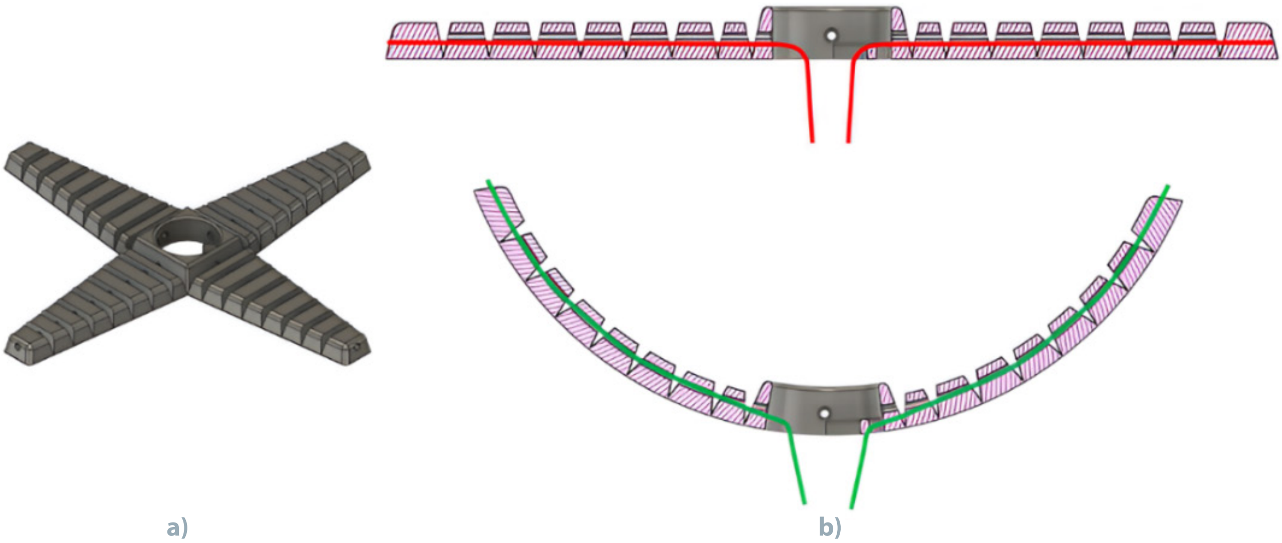

Fig. 7 The design of the flexible clamp: a) General design; b) The opening and closing of the system thanks to the nylon thread system

All elements are joined with screws, which facilitates assembly and disassembly in a matter of minutes. This approach ensured a cost-effective and accessible manufacturing process for future research.

The PLA and aluminium parts are connected via M4 screws and reinforced with printed brackets. The aluminium provides rigidity, while PLA offers flexibility and lightweight construction. This hybrid design ensures sufficient strength without compromising the ease of customisation.

Design and modelling of the flexible gripper

The use of soft materials such as TPU allows not only adaptability but also creates a distributed contact area. Studies in contact mechanics such as Achilli et al. (2022) employed 3D scanning and modelling (Hertz vs JKR) to estimate deformation and contact in silicone pads. Similarly, our design seeks to maximise contact area without concentrating pressure, avoiding damage to the fruit. According to Bac et al. (2014), the typical gripping force required for apples and citrus fruits is 10–30 N. The system delivers a closing force of 288 N, allowing distributed pressure through TPU flexibility, avoiding damage while ensuring firm grip.

The flexible gripper was developed with a focus on flexibility and adaptability, allowing the same system to be used in various harvesting scenarios. Therefore, this prototype focuses on fruits ranging from 0.04 m to 0.012 m in diameter and weighing approximately 0.1 kg to 0.2 kg. This mechanism allows a single servomotor to complete the grip, or up to four servomotors to complete the grip. This decision was made to increase gripping force without compromising the size of the arm, as the servos are driven by nylon threads. The servomotors are located at the base, not at the end of the arm, significantly lightening the mechanism. This configuration also allows the gripping of asymmetrical fruits with only slight programming changes. Figure 7 illustrates the overall structure of the gripper and its operating principle.

Use of TPU in gripper manufacturing

For the construction of the flexible gripper shown in Fig. 8, TPU was chosen, a material used in various 3D printing applications due to its mechanical properties, which provide a good combination of flexibility and strength.

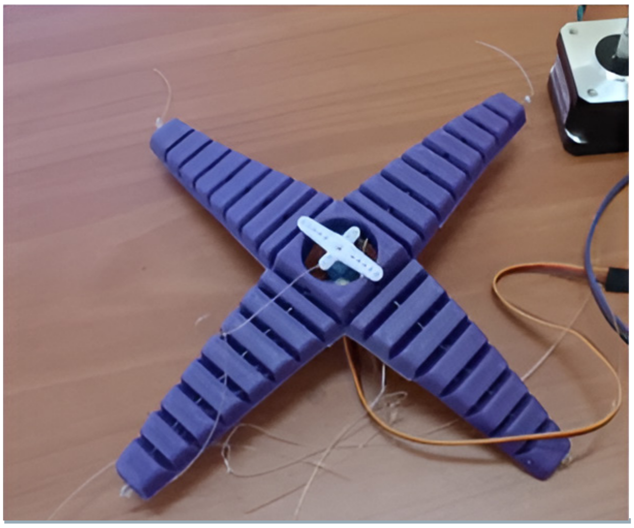

Fig. 8 Flexible gripper constructed from TPU which contracts with the help of servomotors

The gripper, made from a single piece of flexible material, showed great adaptability to different fruit sizes and shapes (within the previously defined range). Simple calibration through programming changes enabled safe and effective gripping in most cases, without the need for specialised sensors. Calibration was performed prior to each test batch. This included adjusting the zero positions of servomotors and fine-tuning the nylon thread tension to ensure synchronised finger motion. This process was critical in improving symmetrical gripping and reducing failure rate (Blanco et al., 2025).

Implementation of the actuation system

The actuation system of the robotic arm consists of NEMA 17 stepper motors for the movement of the base, main arm, and secondary arm, as well as four 360° MG996R servomotors for controlling the flexible gripper. These actuators were selected based on the torque requirements necessary to ensure stable and precise movement while minimising the total weight of the system (Fig. 9).

Torque calculation for the rotation base

The first NEMA 17 motor is located at the base of the arm and is responsible for the rotation along the vertical axis. To calculate the required torque, we consider the length of the fully extended arm 0.518 m and the total weight of the system 2 kg.

The force exerted due to gravity is:

$$F = m \times g = (2\ \text{kg}) \times (9.81\ \text{m·s}^{-2}) = 19.62\ \text{N} \quad (1)$$

The torque required to rotate the arm around the base is:

$$\tau = F \times d = (19.62\ \text{N}) \times (0.5\ \text{m}) = 9.81\ \text{N·m} \quad (2)$$

Given that a single commercial NEMA 17 motor has a maximum torque of 0.45 N·m, this value is insufficient. To compensate for this, a mechanical reduction is employed with a transmission pulley of a 1:8 ratio, which increases the output torque to:

$$\tau_{out} = (0.45\ \text{N·m}) \times 8 = 3.6\ \text{N·m} \quad (3)$$

This value is still not enough to support the weight of the arm and rotate it stably. However, there are techniques that allow achieving the objective without relying on motors with higher torque. The method for rotating the arm was reconsidered, and it no longer rotates when fully extended. Instead, the arm rotates while retracted, which reduces the torque. Therefore, the length taken into account is now 150 mm, thus concentrating almost all the weight at the larger base.

Initial data

Length of retracted arm: 0.150 m
Total mass: 2 kg
Gravitational acceleration: 9.81 m·s^{-2}
NEMA 17 motor torque: 0.45 N·m
Transmission ratio: 8 : 1 (calculated using pulley diameters)

Calculation of gravitational force

The gravitational force exerted is calculated as:

$$F = m \times g = (2\ \text{kg}) \times (9.81\ \text{m·s}^{-2}) = 19.62\ \text{N} \quad (4)$$

Calculation of torque with the new effective distance

The torque required with the new retracted arm length is:

$$\tau = F \times d = (19.62\ \text{N}) \times (0.150\ \text{m}) = 2.94\ \text{N·m} \quad (5)$$

Verification with pulley transmission

The small pulley connected to the motor has a diameter of 0.020 m, giving a radius of 0.010 m. The large pulley has a diameter of 0.160 m, giving a radius of 0.080 m.

Theoretical transmission ratio

The theoretical transmission ratio is calculated as:

$$R_1 = \textit{ratio large pulley/ratio small pulley} = 0.080/0.010 = 8 \quad (6)$$

With a NEMA 17 motor providing 0.45 N·m of torque, the output torque is:

$$\tau_{out} = \tau \times R_1 = 0.45 \times 8 = 3.6\ \text{N·m} \quad (7)$$

Now, with the arm retracted to 0.15 m, the required torque is 2.94 N·m, while the system provides 3.6 N·m.

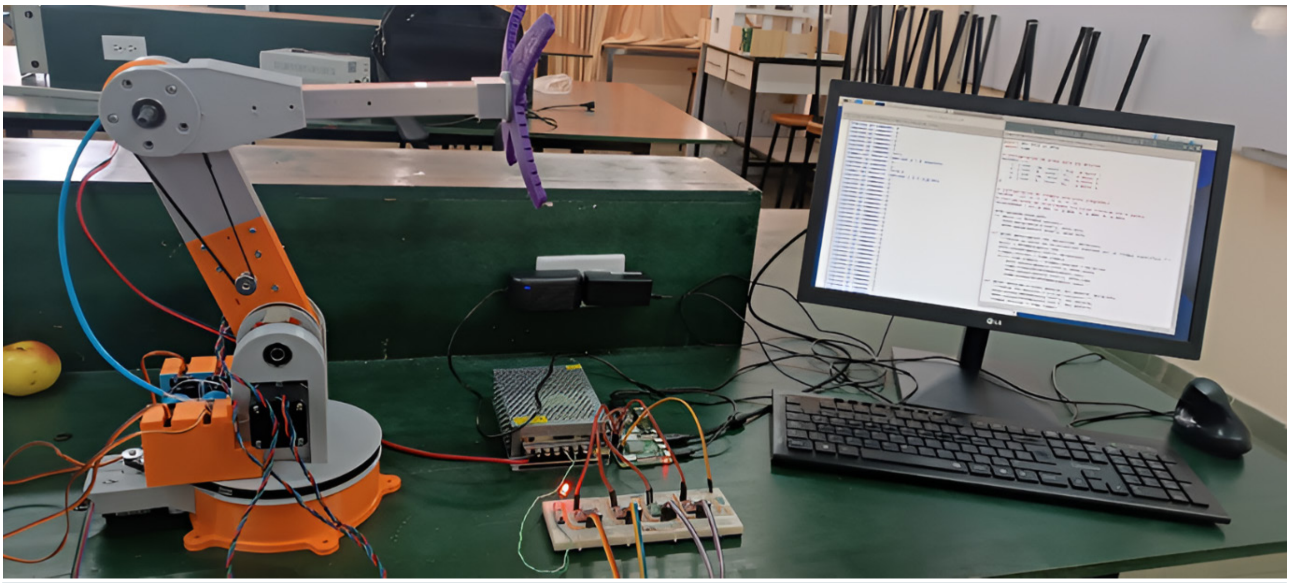

Fig. 9 Complete prototype with its control station made on the Raspberry Pi 4

The system can move without issues, as the output torque exceeds the required torque. The key points are:
- Reducing the arm length to 0.15 m decreases the torque demand.
- The toothed belts transmit torque without slipping losses.
- The output torque 3.6 N·m is sufficient to rotate the base.

Torque calculation for the main arm

The main arm is elevated using two NEMA 17 motors located at its base to distribute the load evenly. The calculation considers half of the total weight of the arm, i.e., 1 kg per motor.

Gravitational force: The force due to gravity is calculated as:

$$F = m \times g = (1\ \text{kg}) \times (9.81\ \text{m·s}^{-2}) = 9.81\ \text{N} \quad (8)$$

Required torque calculation: The arm has an effective length of 500 mm = 0.500 m, so the required torque is:

$$\tau = F \times d = 9.81\ \text{N} \times 0.5\ \text{m} = 4.91\ \text{N·m} \quad (9)$$

Transmission ratio calculation: The theoretical transmission ratio of the pulleys is obtained by dividing their radio:

$$R_2 = \textit{ratio large pulley/ratio small pulley} = 32/10 = 3.2 \quad (10)$$

Output torque with motors: Each NEMA 17 motor provides a torque of 0.45 N·m, but when two motors are used in parallel, the total torque of the system without transmission is:

$$\tau_{mot} = 0.45 \times 2 = 0.90\ \text{N·m} \quad (11)$$

After transmission reduction, the output torque becomes:

$$\tau_{out} = 0.90 \times 3.2 = 2.88\ \text{N·m} \quad (12)$$

The required torque to lift the arm is 4.91 N.m, but the system provides only 2.88 N·m. This means that the available torque is insufficient to safely lift the main arm. However, since the motors cannot be changed, a compensation strategy was implemented by reducing the working range, as was done with the base. The length of the arm was adjusted to 0.280 m.

For an effective length of 0.280 m, the required torque is:

$$\tau = F \times d = 9.81\ \text{N} \times 0.280\ \text{m} = 2.75\ \text{N·m} \quad (13)$$

Therefore, the required torque to lift the arm is 2.75 N·m. The system provides 2.88 N·m, which is sufficient to lift the main arm without any issues.

Torque calculation for the secondary arm: The secondary arm is telescopic and uses a single NEMA 17 motor. Its approximate weight is 0.5 kg, including the gripper mechanism.

Gravitational force: The force due to gravity is calculated as:

$$F = m \times g = (0.5\ \text{kg}) \times (9.81\ \text{m·s}^{-2}) = 4.91\ \text{N} \quad (14)$$

Required torque calculation: For a length of 0.25 m, the required torque is:

$$\tau = F \times d = (4.91\ \text{N}) \times (0.25\ \text{m}) = 1.23\ \text{N·m} \quad (15)$$

Transmission ratio calculation: The theoretical transmission ratio of the pulleys is obtained by dividing their radio:

$$R_3 = \textit{ratio large pulley/ratio small pulley} = 32/10 = 3.2 \quad (16)$$

Output torque with the motor: A 3.2 reduction is applied to increase the motor's torque to:

$$\tau_{out} = 0.45 \times 3.2 = 1.44\ \text{N·m} \quad (17)$$

This value is sufficient to lift the secondary arm without overloading the motor.

Torque calculation for the flexible gripper: The flexible gripper is designed with four flexible tips, each driven by a 360° MG996R servomotor. These motors are located at the base of the arm, minimising the weight at the end of the arm and reducing the torque required in the main motors. Each servomotor generates a torque of 1.08 N·m and acts on a nylon thread that closes the gripper.

Force calculation for each tip: To calculate the force applied at each tip, we consider the radius of the winding drum (r = 0.015 m):

$$F = \tau / r = 1.08\ \text{N·m} / 0.015\ \text{m} = 72\ \text{N} \quad (18)$$

Total closing force: Since there are four servomotors, the total closing force is:

$$F_{total} = 4 \times 72\ \text{N} = 288\ \text{N} \quad (19)$$

This value is sufficient to grip fruits without requiring additional sensors, as the flexibility of the TPU material allows for adjustable gripping pressure. Theoretically, a single motor would suffice; however, four motors are used to allow independent control of each tip, providing greater precision for gripping the fruits.

Testing with fruits of different sizes and textures

All tests were conducted indoors under controlled laboratory conditions with ambient lighting (~500 lux), temperature maintained between 22–24°C, and no airflow. Fruits were manually placed on a platform at a fixed height of 0.3 m relative to the base of the robot. The gripping test was of the ‚pick-and-hold' type: the gripper approached the fruit, attempted to grasp it, and held it firmly for 5 seconds. A successful attempt was defined as the ability to lift and hold the fruit without visible slippage or dropping.

Experimental tests were conducted using fruits with varying characteristics to evaluate the system's performance

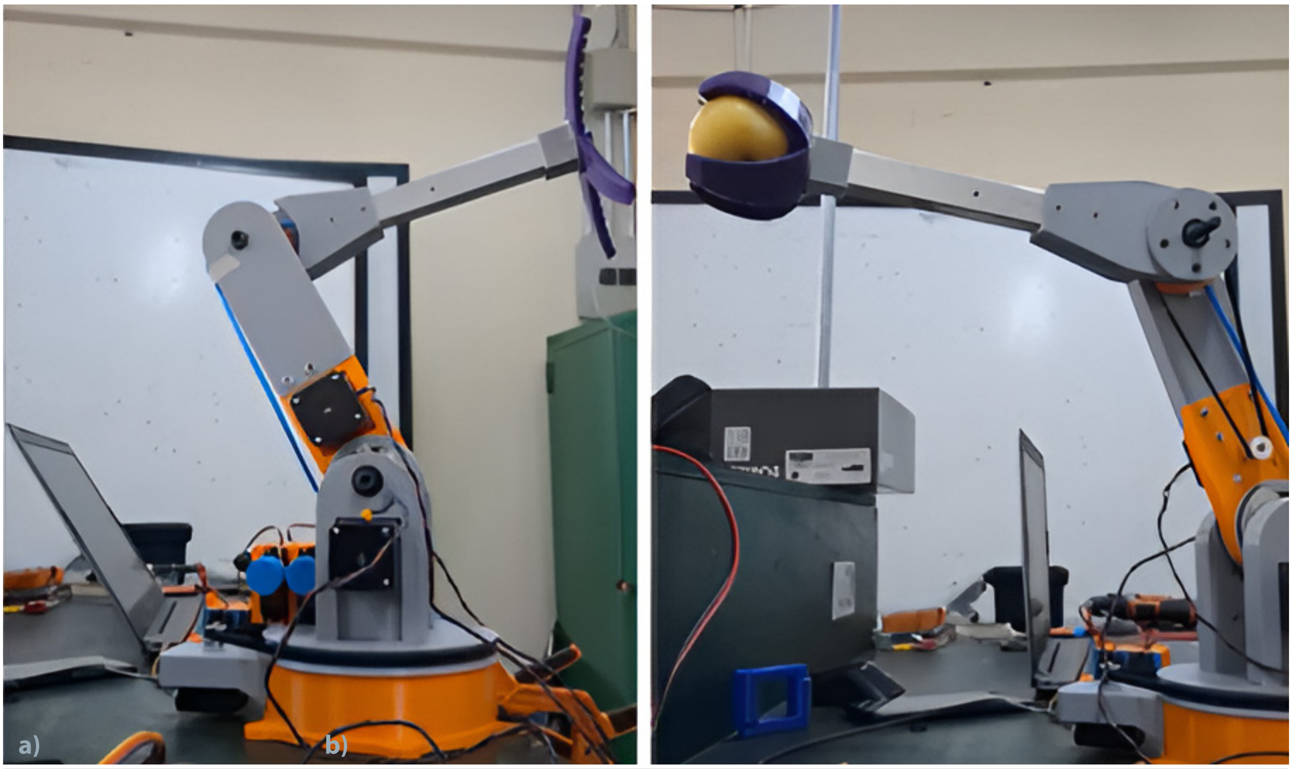

Fig. 10 Harvesting tests performed in laboratories: a) The arm positioning itself; b) The arm harvesting an apple

under real-world conditions. The selected fruits for testing were:

- Apples: With a firm texture and round shape, representing a medium-sized fruit.
- Pears: Irregular in shape with a softer texture, requiring a more delicate grip.
- Citrus fruits: With thicker skin and a slippery surface, presenting an additional challenge for gripping.

For each type of fruit, multiple tests were carried out with different configurations of gripping pressure (Fig. 10).

A total of 30 repetitions were performed for each type of fruit to ensure statistically significant results. The distribution of the trials was as follows:

- 30 attempts for medium-sized apples.
- 30 attempts for medium-sized pears.
- 30 attempts for citrus fruits (lemons, grapefruits).

Statistical analysis of results: To conduct a proper statistical evaluation of the trials, frequency distribution analysis and the calculation of the average success rate for each fruit type were employed.

Success rate calculation: Success data (success = 1, failure = 0):

- Apples: 20 successes out of 30 attempts.
- Pears: 18 successes out of 30 attempts.
- Citrus fruits: 26 successes out of 30 attempts.

$$\textit{success rate for apples} = 20/30 = 0.66 \text{ (or 67\%)} \quad (20)$$

$$\textit{success rate for pears} = 18/30 = 0.60 \text{ (or 60\%)} \quad (21)$$

$$\textit{success rate for citrus fruits} = 26/30 = 0.87 \text{ (or 87\%)} \quad (22)$$

Figure 11 shows a summary of the data obtained for the collection of three different types of fruits comparing their successes and failures.

Figure 12 shows the individual attempts in each test performed (30 in total) in a comparison that shows exactly when the collection process fails.

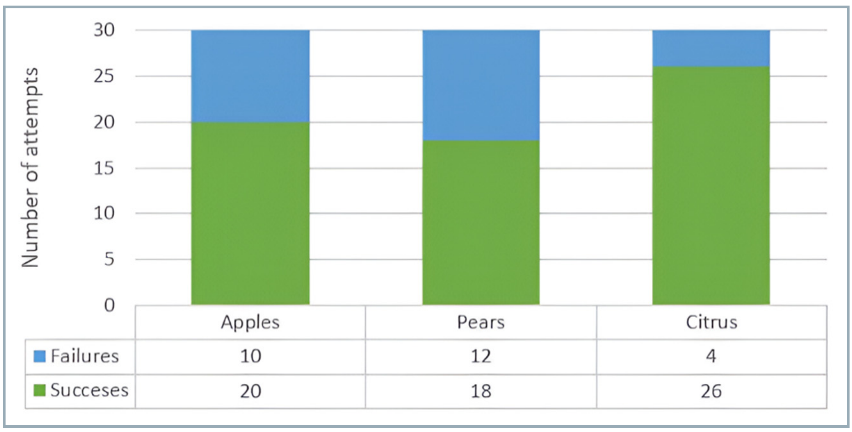

Fig. 11 Summary of successes and failures in the collection of each type of fruit

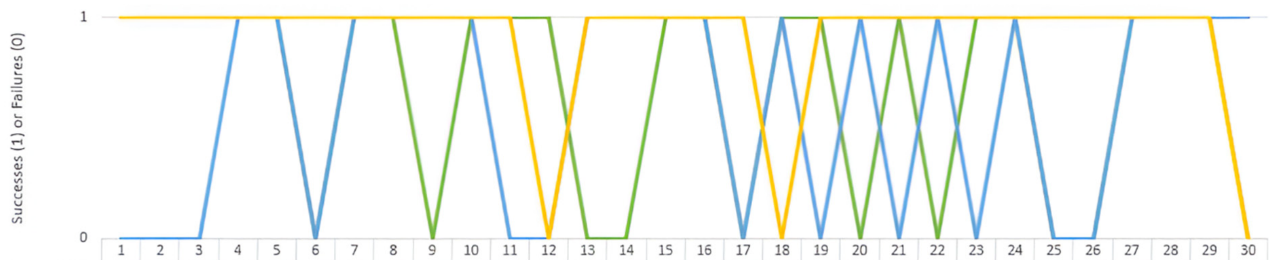

	1	2	3	4	5	6	7	8	9	10	11	12	13	14	15	16	17	18	19	20	21	22	23	24	25	26	27	28	29	30
Apples	1	1	1	1	1	0	1	1	0	1	1	1	0	0	1	1	0	1	1	0	1	0	1	1	0	0	1	1	1	0
Pears	0	0	0	1	1	0	1	1	1	1	0	0	1	1	1	1	0	1	0	1	0	1	0	1	0	0	1	1	1	1
Citrus	1	1	1	1	1	1	1	1	1	1	1	0	1	1	1	1	1	0	1	1	1	1	1	1	1	1	1	1	1	0

Fig. 12 Individual results of successes and failures for each type of fruit

Calculation of the mean and variance

To perform the *t*-test, we first need to calculate the mean ($\bar{X}$): and variance (s^2) of the success rates for each fruit type.
Mean ($\bar{X}$):

$$\bar{X} = \sum X_i / n \tag{23}$$

Variance (s^2):

$$s^2 = \sum \left(X_i - \bar{X}\right)^2 / (n-1) \tag{24}$$

For apples (30 attempts):

$$X_1 = [1, 1, 1, 1, 1, 0, 1, 1, 0, 1, 1, 1, 0, 0, 1, 1, 0, 1, 1, 0, 1, 0, 1, 1, 0, 0, 1, 1, 1, 0]$$

Mean (success rate): 0.67 (67%) Variance: 0.2222
For pears (30 attempts):

$$X_2 = [0, 0, 0, 1, 1, 0, 1, 1, 1, 1, 0, 0, 1, 1, 1, 1, 0, 1, 0, 1, 0, 1, 0, 1, 0, 0, 1, 1, 1, 1]$$

Mean (success rate): 0.60 (60%) Variance: 0.24
For citrus fruits (30 attempts):

$$X_3 = [1, 1, 1, 1, 1, 1, 1, 1, 1, 1, 1, 0, 1, 1, 1, 1, 1, 0, 1, 1, 1, 1, 1, 1, 1, 1, 1, 1, 1, 0]$$

Mean (success rate): 0.87 (87%) Variance: 0.1156

Based on the calculations, it concludes that there is no significant difference between the success rates for apples and pears. However, there is a significant difference between the success rates for apples and citrus, and between pears and citrus. These results suggest that the gripper's performance varies significantly when handling citrus fruits, possibly due to their texture or shape characteristics, while the system performs more uniformly with apples and pears.

Application of the *t*-test

Now, we can apply the independent samples *t*-test to compare the differences in success rates between the two fruit groups. In this case, we will make comparisons between apples and pears, apples and citrus, and pears and citrus.

Comparison of apples vs pears: For apples (group 1) and pears (group 2), we have the following values: $X_1 = 0.66$, $X_2 = 0.60$, $s_1^2 = 0.224$, $s_2^2 = 0.233$, and $n_1 = n_2 = 30$. Using these, the *t*-value is calculated as $t = 0.485$.

Comparison of apples vs citrus: For apples (group 1) and citrus (group 2), the values are: $X_1 = 0.66$, $X_2 = 0.87$, $s_1^2 = 0.224$, $s_2^2 = 0.10$, and $n_1 = n_2 = 30$. The *t*-value is $t = -2.02$.

Comparison of pears vs citrus: For pears (group 1) and citrus (group 2), we have: $X_1 = 0.60$, $X_2 = 0.87$, $s_1^2 = 0.233$, $s_2^2 = 0.10$, and $n_1 = n_2 = 30$. The calculated *t*-value is $t = -2.56$.

Interpretation of results

With these *t*-values, we compare the results with the critical *t*-values from the *t*-table to determine whether the differences are significant. Let's assume we are working with a significance level of 0.05 and 58 degrees of freedom (since we are using 30 attempts per group, $n - 1 = 29$ for each group, and the total degrees of freedom are $29 + 29 = 58$):

– Significance level of 0.05: There is a 5% chance of committing a Type I error, and the null hypothesis is rejected if the *p*-value is less than 0.05.
– 58 degrees of freedom: These are used to determine the critical *t*-value to decide whether the calculated *t*-value is significant. With more degrees of freedom, the critical *t*-value decreases, making it easier to reject the null hypothesis when there is a significant difference.
– The critical *t*-value for 58 degrees of freedom and a significance level of 0.05 (two-tailed) is approximately 2.001.

Comparisons

Apples vs pears: $t = 0.485$, which is less than 2.001
Apples vs citrus: $t = -2.02$, which is less than -2.001
Pears vs citrus: $t = -2.56$, which is less than -2.001

Based on the calculations, we conclude that there is no significant difference between the success rates for apples and pears. However, there is a significant difference between the success rates for apples and citrus, and between pears and citrus.

These results suggest that the gripper's performance varies significantly when handling citrus fruits, possibly due to their texture or shape characteristics, while the system performs more uniformly with apples and pears.

Results and discussion

In the experimental tests conducted with the gripper prototype, the system's ability to grasp fruits of different sizes and textures – apples, pears, and citrus fruits – was evaluated. The results showed a high success rate in tests with citrus fruits (87%), followed by apples (67%) and pears (60%). This suggests the gripper is effective in adapting to different fruit shapes and sizes without additional sensors.

The success rates with apples and citrus fruits were considerably high, validating the system's ability to adjust to different fruit sizes with simple servo calibration. However, the results for pears showed the gripper's flexibility may require fine-tuning for certain fruit sizes or shapes.

The experiments were conducted in a controlled laboratory setting, where external conditions such as lighting, wind, humidity, and variability in fruit arrangement were not considered. While the results demonstrate the system's viability in terms of gripping and precision, its performance in a real agricultural setting has not been evaluated.

Based on the statistical analysis, there is no significant difference between the success rates for apples and pears. However, there is a significant difference between the success rates for apples and citrus, and between pears and citrus. These results suggest that the gripper's performance varies significantly when handling citrus fruits, possibly due to their texture or shape characteristics, while the system performs more uniformly with apples and pears.

To provide a compact overview of the experimental outcomes, Table 3 summarises the success rates, mean positional error, and repeatability obtained for each fruit type. This table integrates gripping performance with positioning metrics, offering a clear comparison across the three tested fruits.

Table 3 Technical parameters of the arm

Fruit type	Success rate (%)	Mean positional error (mm)	Repeatability (± mm)
Citrus	87	3.2	2
Apples	67	3.2	2
Pears	60	3.2	2

Positional accuracy and repeatability tests indicated a mean positioning error of 3.2 mm and a repeatability within ±2 mm. These values are within the tolerance requirements reported in the literature for effective fruit harvesting and demonstrate that the arm can reliably return to target positions, an essential factor for consistent fruit picking performance.

The evaluation of the system's gripping capacity was generally positive, with reliable ability to grip apples and citrus fruits within the established range. The system demonstrated excellent adaptability due to the gripper's flexibility, adjusting to various sizes without additional sensors. The distribution of forces, optimised through the design geometry, ensured the fruit was held securely without causing damage.

In tests with pears, although the success rate was lower, the system gripped the fruit correctly in most attempts. This suggests the variability in texture or shape of pears may have affected grip effectiveness, but could be resolved by adjusting calibration parameters.

Compared to other reported works, such as Navas et al. (2024) with a 75% success rate for small fruits using sensor-assisted gripping, and Elfferich et al. (2022) reporting rates between 60–70% with complex sensory systems, the proposed design achieves similar or superior performance – particularly with citrus – despite being a sensorless system. This highlights the effectiveness of careful mechanical design and material choice as a means to reduce system complexity and cost.

These findings are consistent with, and in some cases exceed, the performance ranges (55–75% success rate) reported for current robotic harvesting systems in the literature. In particular, the 87% success rate achieved for citrus fruits represents a significant improvement over the typical figures mentioned in the Introduction, demonstrating that a low-cost, sensorless solution can match or surpass more complex commercial and research systems.

The limitations of the current evaluation include testing only in indoor, controlled conditions with manually placed fruits, not considering environmental factors such as wind, varying illumination, or irregular fruit positioning. Future work should address these factors to validate performance in real-world agricultural settings.

Conclusion

The prototype built for fruit harvesting using a robotic arm and a flexible gripper presents an innovative approach. The results obtained after extensive testing demonstrated a satisfactory performance for an initial prototype. Torque calculations validated the component selection, although high-load situations may require more powerful motors or adjustments to force distribution.

This study demonstrated that a low-cost, sensorless robotic arm can achieve competitive or superior performance to more complex systems, particularly in harvesting citrus fruits, by leveraging careful mechanical design and material selection. The modular structure and 3D-printed components allow rapid adaptation to other fruit types or similar agricultural tasks.

While the robotic arm and gripper performed well in laboratory conditions, testing in realistic environments is necessary. External factors such as arm movement from uneven terrain and variability in stem resistance could affect performance.

Limitations include the exclusive evaluation in indoor, controlled conditions, without environmental stressors such as wind, changing light, or rain, and the absence of automated fruit detection. To validate the prototype in real-world conditions, field tests with different crop varieties are recommended, considering the parameters such as success rate under varying environmental conditions, adaptability to fruit size and firmness, and the impact of climate on performance.

In summary, the robotic arm developed in this study proved to be a highly functional first prototype with strong potential for agricultural automation. Its design principles could be applied in other robotics fields involving object manipulation in unstructured environments or handling fragile objects unsuitable for conventional grippers.

Unsuccessful gripping was primarily observed with pears, likely due to their irregular shape and variable firmness, which created inconsistent contact surfaces. In contrast, citrus fruits, with more uniform geometry and a firmer outer peel, allowed more consistent pressure distribution by the gripper.

Acknowledgement

The authors wish to express their gratitude to the Instituto Tecnológico Superior Rumiñahui for its generous support and sponsorship of this research. Their contributions were invaluable in facilitating the development of the project, the results of which are presented in this article. Financial and logistical support was crucial, including the use of Autodesk Fusion software for the design and modelling of the prototype, as well as the resources provided for 3D printing of the components. This support has been crucial in driving the development of the harvesting robot.

References

Achilli, G.M., Logozzo, S., Malvezzi, M., Valigi, M.C., 2022. Contact mechanics analysis of a soft robotic fingerpad. Frontiers in Mechanical Engineering 8, 966335. https://doi.org/10.3389/fmech.2022.966335

Afsah-Hejri, L., Homayouni, T., Toudeshki, A., Ehsani, R., Ferguson, L., Castro-García, S. 2022. Mechanical harvesting of selected temperate and tropical fruit and nut trees. Horticultural Reviews 49, 171–242. https://doi.org/10.1002/9781119851981.ch4

Alaaudeen, K.M., Selvarajan, S., Manoharan, H., Jhaveri, R.H., 2024. Intelligent robotics harvest system process for fruits grasping prediction. Scientific Reports 14, 2820. https://doi.org/10.1038/s41598-024-52743-8

An, Z., Wang, C., Raj, B., Eswaran, S., Raffik, R., Debnath, S., Rahin, S.A., 2022. Application of new technology of intelligent robot plant protection in ecological agriculture. Journal of Food Quality, 2022, 1–7. https://doi.org/10.1155/2022/1257015

Bac, C.W., Van Henten, E.J., Hemming, J., Edan, Y., 2014. Harvesting robots for high-value crops: state-of-the-art review and challenges ahead. Journal of Field Robotics 31(6), 888–911. https://doi.org/10.1002/rob.21525

Bao, Y., Yuan, N., Zhao, Y., Wu, L. 2022. Recent patents for collection device of fruit harvesting machine. Recent Patents on Engineering 16(4), 96–108. https://doi.org/10.2174/1872212116666220107115125

Baur, P., Iles, A., 2023. Replacing humans with machines: a historical look at technology politics in California agriculture. Agriculture and Human Values 40(1), 113–140. https://doi.org/10.1007/s10460-022-10341-2

Blanco, K., Navas, E., Rodríguez-Nieto, D., Emmi, L., Fernández, R., 2025. Design and experimental assessment of 3D-printed soft grasping interfaces for robotic harvesting. Agronomy, 15(4), 804. https://doi.org/10.3390/agronomy15040804

Buzzatto, J., Jiang, H., Liang, J., Busby, B., Lynch, A., Godoy, R.V., Matsunaga., S., Haraguchi, R., Mariyama, T., MacDonald, B.A., Liarokapis, M., 2024. Multi-layer, sensorized kirigami grippers for delicate yet robust robot grasping and single-grasp object identification. IEEE Access 12, 115994–116012. https://doi.org/10.1109/ACCESS.2024.3446729

Davidson, J.R., Silwal, A., Hohimer, C.J., Karkee, M., Mo, C., Zhang, Q., 2016. Proof-of-concept of a robotic apple harvester. In 2016 IEEE/RSJ International Conference on Intelligent Robots and Systems (IROS), pp. 634–639. IEEE, Daejeon, South Korea. https://doi.org/10.1109/IROS.2016.7759119

De Grandpré, A., Elton, C., Senese, D., Mullinix, K., 2022. Soft adaptation: The role of social capital in building resilient agricultural landscapes. Frontiers in Agronomy, 4. https://doi.org/10.3389/fagro.2022.980888

Elfferich, J.F., Dodou, D., Della Santina, C., 2022. Soft robotic grippers for crop handling or harvesting: a review. IEEE Access 10, 75428–75443. https://doi.org/10.1109/ACCESS.2022.3190863

Genbach, A., Jamankulova, N., Beloev, H., Iliev, I., 2018. Energy divider with insert for heat protection of fruit trees. Acta Technologica Agriculturae, 21(1), 8–13. https://doi.org/10.2478/ata-2018-0002

Harman, H., Sklar, E.I., 2022. Multi-agent task allocation techniques for harvest team formation. In Dignum, F., Mathieu, P., Corchado, J.M., De La Prieta, F. (Eds), Advances in Practical Applications of Agents, Multi-Agent Systems, and Complex Systems Simulation. The PAAMS Collection. PAAMS 2022. Lecture Notes in Computer Science 13616. Springer, Cham, Switzerland. https://doi.org/10.1007/978-3-031-18192-4_18

Hasanshahi, B., Cao, L., Song, K.-Y., Zhang, W., 2024. Design of soft robots: A review of methods and future opportunities for research. Machines, 12(8), 527. https://doi.org/10.3390/machines12080527

Kashkarov, A., Diordiiev, V., Sabo, A., Novikov, G., 2018. Semi-autonomous drone for agriculture on the tractor base. Acta Technologica Agriculturae, 21(4), 149–152. https://doi.org/10.2478/ata-2018-0027

Magistri, F., Pan, Y., Bartels, J., Behley, J., Stachniss, C., Lehnert, C., 2024. Improving robotic fruit harvesting within cluttered environments through 3D shape completion. IEEE Robotics and Automation Letters 9(8), 7357–7364. https://doi.org/10.1109/LRA.2024.3421788

Navas, E., Shamshiri, R.R., Dworak, V., Weltzien, C., Fernández, R., 2023. Soft gripper for small fruits harvesting and pick and place operations. Frontiers in Robotics and AI 10, 1330496. https://doi.org/10.3389/frobt.2023.1330496

Spagnuolo, M., Todde, G., Caria, M., Furnitto, N., Schillaci, G., Failla, S., 2025. Agricultural robotics: a technical review addressing challenges in sustainable crop production. Robotics 14(2), 9. https://doi.org/10.3390/robotics14020009

Zhang, J., Kang, N., Qu, Q., Zhou, L., Zhang, H., 2024. Automatic fruit picking technology: a comprehensive review of research advances. Artificial Intelligence Review 57, 54. https://doi.org/10.1007/s10462-023-10674-2